A&A 633, A45 (2020)
https://doi.org/10.1051/0004-6361/201935132

Astronomy & Astrophysics

A strange star scenario for the formation of isolated millisecond pulsars

Long Jiang[1,2,3], Na Wang[1], Wen-Cong Chen[2,3], Xiang-Dong Li[3], Wei-Min Liu[2], and Zhi-Fu Gao[1]

[1] Xinjiang Astronomical Observatory, CAS, Urumqi, Xinjiang 830011, PR China
e-mail: na.wang@xao.ac.cn
[2] School of Physics and Electrical Information, Shangqiu Normal University, Shangqiu, Henan 476000, PR China
e-mail: chenwc@pku.edu.cn
[3] Key laboratory of Modern Astronomy and Astrophysics, Nanjing University, Ministry of Education, Nanjing 210046, PR China
e-mail: lixd@nju.edu.cn

Received 25 January 2019 / Accepted 17 November 2019

ABSTRACT

According to the recycling model, neutron stars in low-mass X-ray binaries were spun up to millisecond pulsars (MSPs), which indicates that all MSPs in the Galactic plane ought to be harbored in binaries. However, about 20% Galactic field MSPs are found to be solitary. To interpret this problem, we assume that the accreting neutron star in binaries may collapse and become a strange star when it reaches some critical mass limit. Mass loss and a weak kick induced by asymmetric collapse during the phase transition (PT) from neutron star to strange star can result in isolated MSPs. In this work, we use a population-synthesis code to examine the PT model. The simulated results show that a kick velocity of $\sim$60 km s^{-1} can produce $\sim 6 \times 10^3$ isolated MSPs and birth rate of $\sim 6.6 \times 10^{-7}$ yr^{-1} in the Galaxy, which is approximately in agreement with predictions from observations. For the purpose of comparisons with future observation, we also give the mass distributions of radio and X-ray binary MSPs, along with the delay time distribution.

Key words. stars: evolution – stars: neutron – pulsars: general

1. Introduction

According to the widely accepted standard recycling model (Alpar et al. 1982; Radhakrishnan & Srinivasan 1982; Bhattacharya & van den Heuvel 1991), millisecond pulsars (MSPs) which are characterized by short spin periods ($P_{\rm spin} \leq 30$ ms) and low surface magnetic fields ($B \sim 10^8$–10^9 G) evolved from neutron star (NS) low-mass X-ray binaries (LMXBs; Manchester 2004; Lorimer 2008). Donor stars in LMXBs with initial orbital periods near or less than the so-called bifurcation period (Pylyser & Savonije 1989) always lose their hydrogen envelope and evolve into low-mass He white dwarfs (WDs). Considering the circularization due to the tidal interaction during the mass transfer, most MSPs should be located in binary systems with highly circularized orbits (Phinney 1992), except for those MSPs in dense globular clusters, which may form via some dynamical processes (Verbunt et al. 1987; Verbunt 1988). However, about 20% of MSPs are isolated in the Galactic field, which is difficult to understand. Since the predicted birth rate of Galactic MSPs is $\gtrsim 3 \times 10^{-6}$ yr^{-1} (Lorimer 1995; Lyne et al. 1998; Ferraio & Wickramasinghe 2007; Story et al. 2007), the birth rate of isolated MSPs should be $\gtrsim 6 \times 10^{-7}$ yr^{-1}.

To solve this problem, van den Heuvel & van Paradijs (1988) and Kluzniak et al. (1988) proposed that the donor stars may have been ablated by the γ-ray and energetic particles emitted by the MSPs just as happening in PSR B1957+20 (Fruchter et al. 1988). It seems that this scenario is supported by the discoveries of MSP+planet binaries (Wolszczan & Frail 1992) and of PSR B1937+21, which was found to be orbited by an asteroid belt with total mass $\leq$0.05 earth mass (Shannon et al. 2013). The belt of B1937+21 was thought to be made up of the debris of its former companion which had been tidally disrupted. However, other studies show that the evaporation timescale may be too long (Chen et al. 2013) unless a very high evaporation efficiency ($\sim$0.1) is adopted (Jia & Li 2016).

Decades ago, the concept of the strange star (SS) was proposed (Itoh 1970; Bodmer 1971; Farhi & Jaffe 1984; Witten 1984; Alcock et al. 1996; Haensel et al. 1986). It was suggested that some of the pulsars may be SSs rather than NSs since the strange quark matter may be the most stable state of matter. Some researchers argued that NSs and SSs may coexist in nature and when the central density of an NS rises above the critical density for quark deconfinement, NS-SS phase transition (PT) may occur (Bombaci & Datta 2000; Berezhiani et al. 2003; Bombaci et al. 2004, 2008, 2016; Bhattacharyya et al. 2017). Olinto (1987) and Horvath & Benvenuto (1988) suggest that the process of PT is gradual, lasting around 10^8 yr. However, Cheng & Dai (1996) and Ouyed et al. (2002) argue that the process might take place in a detonation mode and the released energy is compatible with a core collapse supernova (CCSN).

In the present paper, based upon the idea that accreting NSs in LMXBs may reach some critical mass limit and transit to SSs promptly, we propose that the NS-SS PT with a kick velocity may account for the formation of isolated MSPs. The details of the scenario and the population-synthesis code are described in Sects. 2 and 3, respectively. Simulated results are given in Sect. 4, while some discussions about this scenario are presented in Sect. 5. Finally, we make a brief summary in Sect. 6.

2. Strange star scenario

At present, the detailed processes for the dissolution of baryons into their quark constituents are not well understood. Based on the standard equation of state (EoS) of neutron-rich matter, Staff et al. (2006) proposed that the critical density for quark deconfinement is $\rho_c \sim 5\rho_0$, where $\rho_0 \sim 2.7\times10^{14}\,\mathrm{g\,cm^{-3}}$ is the nuclear saturation density. If the NS is fast-spinning, the central density might be centrifugally diluted. The maximum mass of NS with an angle velocity $\Omega = 2\pi/P$ can be expressed as (Hartle 1970; Baym et al. 1971):

$$M_c(\Omega) = M_c(0) + \delta M(\Omega/\Omega_{\max})^2, \quad (1)$$

where $\Omega_{\max}$ is the maximum angular velocity (in this work, we take $\Omega_{\max} = 2000\pi\,\mathrm{rad\,s^{-1}}$, e. g., the minimum spin period $P_{\min} = 1\,\mathrm{ms}$); $M_c(0)$ is the maximum mass of the non-rotating NS, δM represents the difference between $M_c(0)$ and M_c. Lasota et al. (1996) showed that rigid rotation can increase the maximum mass of NS by a fraction of 20%, while Morrison et al. (2004) found that the fraction for a differentially rotating NS is ≤50%. Haensel & Yakovlev (2007) predicted that the maximum baryon mass of differentially rotating NSs is ≥50% higher than that of non-rotating NS. In our simulation, we take $M_c(0) = 1.8\,M_\odot$ according to Akmal et al. (1998) and $\delta M = 0.4\,M_\odot$, similarly to Lasota et al. (1996). If the mass of the NS exceeds the maximum mass, for example, $M_{\rm NS} \geq M_c(\Omega)$, PT is assumed to take place.

In the recycling stage, the NS would accrete the material from the donor star. We adopt a description for the spin period evolution of the NS given by Cheng & Zhang (2000):

$$P = \max\left[1.1\left(\frac{M-M_{\rm NS,i}}{M_\odot}\right)^{-1} R_6^{-5/14} I_{45}\left(\frac{M}{M_\odot}\right)^{-1/2}, 1.1\left(\frac{M}{M_\odot}\right)^{-1/2} R_6^{17/14}\right]\mathrm{ms}, \quad (2)$$

where R_6 is the radius of the NS in units of 10^6 cm, and I_{45} is the moment of inertia of the NS in units of $10^{45}\,\mathrm{g\,cm^2}$ ($R_6 = I_{45} = 1$ in our simulation); M and $M_{\rm NS,i}$ are the current and initial masses of the NS, respectively. If the spin period of the NS is less than 10 ms, a MSP is assumed to form.

Some researchers studied the difference between the gravitational mass of NS and SS (for different EoS) with the same baryon number (Bombaci & Datta 2000; Drago et al. 2007; Marquez & Menezes 2007). They obtained the similar results: for NS with a mass of ∼1.5 $M_\odot$, $M_{\rm NS} - M_{\rm SS} \approx 0.15\,M_\odot$[1]. According to their research, the mass loss ratio $(M_{\rm NS}-M_{\rm SS})/M_{\rm NS}$ during PT is about 0.1. Assuming that this ratio is suitable for all NS-SS PT, in this work, we take $\Delta M = M_{\rm NS} - M_{\rm SS} = 0.1 M_{\rm NS}$.

Following the study of Cheng & Dai (1996) and Ouyed et al. (2002), we consider that the PT in the core of NS takes place quickly, as with CCSN, and a kick velocity V_k is imparted to the newly born SS. The orbital parameters change during PT can be solved following Hills (1983), Dewi & Pols (2003), Shao & Li (2016). Due to long duration of mass transfer, the binary orbit before PT is assumed to be circular. The positional angle of V_k with respect to the pre-PT orbital plane is set to be ϕ and the angle between V_k and the pre-PT orbital velocity $V_0 (= (2\pi G M_0/P_{\rm orb,0})^{1/3})$ is θ. The ratio between the semi-major axes before and after PT is:

$$\frac{a_0}{a} = 2 - \frac{M_0}{M_0 - \Delta M}(1 + \nu + 2\nu\cos\theta), \quad (3)$$

where $\nu = V_k/V_0$, M_0 and $P_{\rm orb,0}$ are the total mass and the orbital period of the binary before PT, respectively. Due to the influence of mass loss and kick, the eccentricity after PT can be written as:

$$1 - e^2 = \frac{a_0 M_0}{a(M_0-\Delta M)}[1 + 2\nu\cos\theta + \nu^2(\cos^2\theta + \sin^2\theta\sin^2\phi)]. \quad (4)$$

For specific kick velocities and angles mentioned above, the PT process can disrupt the binary system and result in the birth of isolated MSPs.

3. Population synthesis

To study the total number and birth rate of isolated MSPs formed via NS-SS PT process in the Galaxy and the initial parameter-space of the progenitors, we use the rapid binary star evolution (BSE) code, which was developed by Hurley et al. (2000, 2002). Our main modifications of the code are as follows.

3.1. Modification for SS

In the original code, the types of stars were noted with 16 integer numbers (kw) from 0 to 15, where 13 is for NS and 14 is for BH (Hurley et al. 2000). The maximum mass of NS is 3.0 $M_\odot$. If the mass of a NS exceeds this limit during the accretion process, kw will become 14. Based on the description mentioned in the previous section, we introduce a new star type for SS when the mass of NS is large enough, that is, $M_{\rm NS} \geq M_c(\Omega)$, and we change the integer type number kw from 13 (for NS) to 99 (for SS).

Considering the mass accretion of SS in binaries, there is a maximum mass of SS, $M_{\rm SS,MAX}$, for an object with mass beyond which it is assumed to collapse to a black hole, and kw will change to 14. Glendenning (2000) studied the MIT bag model with different bag parameter B and obtained a maximum mass of ∼2.2 $M_\odot$ and ∼1.7 $M_\odot$ for $B^{1/4} = 140$ MeV and $B^{1/4} = 160$ MeV, respectively. Gangopadhyay et al. (2013) explored the density dependent quark mass model which was developed by Dey et al. (1998) and obtained an upper limit of ∼2.0 $M_\odot$. However, Lai & Xu (2009) propose that a massive quark star of ∼5 $M_\odot$ is also stable for the EoS of Lennard-Jones quark matter. The maximum mass of SS strongly depends on EoS, hence, it is still a controversial topic. Furthermore, the spin evolution also influences the maximum mass of SS like NS. In this work, we take a fixed value of $M_{\rm SS,MAX} = 2.5\,M_\odot$ in the standard model. To study its influence, a larger value $M_{\rm SS,MAX} = 3.0\,M_\odot$ is also used (Zhu et al. 2013).

3.2. Initial input parameters

In the simulation, the initial parameters are set following Liu & Li (2007) and Chen et al. (2011). We assume that all stars are born in binary systems with a solar metallicity ($Z = 0.02$) and circular orbits ($e = 0$). In the Galaxy, one binary with primary mass $M_1 \geq 0.8\,M_\odot$ is thought to be born per year, thus, a constant star formation rate $S = 7.6085\,\mathrm{yr^{-1}}$ is adopted (Hurley et al. 2002). Using the initial mass function $f(M_1)$ given by Kroupa et al. (1993), the mass distribution of the primary is

[1] A low value is also possible; for example, Schaffner-Bielich et al. (2002) suggested that the difference in the gravitational mass between NS and hyperon star is ∼0.03 $M_\odot$.

Table 1. Input parameters of different models.

Model	λ	$\alpha_{\rm CE}$	$\sigma_{\rm PT}$	$M_{\rm SS,MAX}$	$f_{\rm acc}$
A	0.5	3	60	2.5	0.5
B	0.5	1	60	2.5	0.5
C	0.5	3	20	2.5	0.5
D	0.5	3	100	2.5	0.5
E	NJU*	3	60	2.5	0.5
F	NJU	1	60	2.5	0.5
G	0.5	3	60	3.0	0.5
I	0.5	3	60	2.5	0.3
J	0.5	3	60	2.5	0.8

Notes. Results from researchers of Nanjing university, Xu & Li (2010a,b) and Wang et al. (2016). See the text for details.

set to $\Phi(\ln M_1) = M_1 f(M_1)$. The mass distribution of the secondary is $\Phi(\ln M_2) = M_2/M_1 = q$, where q is the mass ratio, corresponding to a uniform distribution from 0 to 1. The binary separation a is assumed to follow a uniform distribution of $\ln a$, that is, $\Phi(\ln a) = k$ where $k = 0.12328$, following Hurley et al. (2002). The input parameter space for M_1, M_2, and a are set to be 0.8−80 $M_\odot$, 0.1−80 $M_\odot$, 3−10 000 $R_\odot$, respectively. Setting $n_X(= 200)$ grid points in logarithmic space, we get

$$\delta \ln X = \frac{\ln X_{\rm max} - \ln X_{\rm min}}{n_X - 1}, \tag{5}$$

where X indicates M_1, M_2 and a.

3.3. Common envelope evolution

As a result of ROLF, the binary probably enters a common envelope (CE) phase. Because this process is very complicated and uncertain, we adopt an energy mechanism (Hurley et al. 2002). The binding energy of the envelope is:

$$E_{\rm bind} = \frac{G M_{\rm d} M_{\rm d,e}}{\lambda R_{\rm L}}, \tag{6}$$

where $M_{\rm d}$ and $M_{\rm d,e}$ are the total mass and the envelope mass of the donor star, respectively; $R_{\rm L}$ is the Roche lobe radius, $\lambda(< 1)$ is the binding energy parameter which denotes the mass distribution in the envelope (Webbink 1984; de Kool 1990). The parameter λ for different stars had already been systematically calculated by Dewi & Tauris (2000), Podsiadlowski et al. (2003), Xu & Li (2010a,b) and Wang et al. (2016) In this work, we adopt a fixed $\lambda = 0.5$ following (Tout et al. 1997).

The efficiency parameter which describes the fraction of orbital energy transferred to expel the envelope during the CE evolution is $\alpha_{\rm CE} = E_{\rm bind}/(E_{\rm orb,f} - E_{\rm orb,i})$ (Hurley et al. 2002), where $E_{\rm orb,i}$ and $E_{\rm orb,f}$ are the initial and the final orbital energy of the core, respectively. In our standard model, $\alpha_{\rm CE} = 3$ is adopted following Hurley et al. (2010), while a lower value of $\alpha_{\rm CE} = 1$ is also used.

3.4. Kick velocity

The kick velocity distribution during CCSN or PT, which may arise from the asymmetric collapses, can be described by a Maxwellian distribution with one-dimensional rms σ. Hobbs et al. (2005) made a statistical study of the proper motion of 233 pulsars. Their study for 73 young pulsars with characteristic age less then 300 Myr indicated $\sigma_{\rm CC} = 265\,{\rm km\,s^{-1}}$. Since the one-dimensional mean speed of recycled pulsars in their study is $54(6)\,{\rm km\,s^{-1}}$, we set $\sigma_{\rm PT} = 60\,{\rm km\,s^{-1}}$ in our simulation, while some lower and higher speeds are also used for comparison.

3.5. RLOF mass transfer

After the primary evolves into an NS, the secondary will evolve to fill its Roche lobe and trigger the mass transfer. The material from the secondary is transferred to the NS at a rate of $\dot{M}_2$. The accretion rate ($\dot{M}_{\rm NS}$) of the NS (also subsequent SS after PT) is thought to be limited to the so-called Eddington accretion rate $\dot{M}_{\rm Edd}$ and an accretion efficiency $f_{\rm acc}$, that is,

$$\dot{M}_{\rm NS} = \min[\dot{M}_{\rm Edd}, f_{\rm acc}|\dot{M}_2|]. \tag{7}$$

In our simulation, we adopt $f_{\rm acc} = 0.3$, 0.8, and 0.5 (Podsiadlowski et al. 2002). The mass loss is thought to be ejected in the vicinity of the NS in the form of isotropic winds, carrying the specific angular momentum of the NS.

We calculate the evolution of each binary up to an age of 12 Gyr using the BSE code. During the evolution of binary systems, if a NS evolves into a SS MSP (isolated SS MSP or binary SS MSP), it makes a contribution to the birth rate (in units of systems per year) of relevant MSPs as

$$\delta r = S\,(\Phi \ln M_1)(\Phi \ln M_2)(\Phi \ln a)\delta \ln M_1 \delta \ln M_2 \delta \ln a. \tag{8}$$

If this kind of SS lives for a time of δt, it makes a contribution to the number

$$\delta n = \delta r \delta t. \tag{9}$$

Besides the assumptions mentioned above, we also consider other binary star interactions, such as the mass transfer, accretion via stellar winds, tidal friction, and orbital angular momentum loss via gravitational wave radiation and magnetic braking (Hurley et al. 2002).

4. Simulation results

Based on the assumptions mentioned above, we simulated the evolution of $n_{\rm X}^3(= 8\times10^6)$ binaries. We constructed several models with the input parameters shown in Table 1. In our standard model, Model A, $\lambda = 0.5$, $\alpha_{\rm CE} = 3$, $\sigma_{\rm PT} = 60\,{\rm km\,s^{-1}}$, $M_{\rm SS,MAX} = 2.5\,M_\odot$ and $f_{\rm acc} = 0.5$.

4.1. Predicted numbers and birth rates

The predicted numbers and birth rates of different types of SS MSPs (radio, X-ray, with different companion types, and isolated MSPs) in each model are summarized in Table 2. Some main results are summarized as follows:

(1) The birth rate and the total number of isolated SS MSPs in the Galaxy predicted by Model A is $\sim 6.6\times10^{-7}\,{\rm yr^{-1}}$ and 5878, respectively, which is consistent with the lower limit predicted by Lorimer (1995), Lyne et al. (1998), Ferraio & Wickramasinghe (2007) and Story et al. (2007).

(2) Models B, E and F yield a relatively low birth rate and total number, implying that binding energy parameter λ and $\alpha_{\rm CE}$ play an important role in forming various SS MSPs. A higher $\alpha_{\rm CE}$ can prevent the binaries from coalescence during the CE phase, enhancing the birth rate of the post-CE binaries significantly (Liu & Li 2006).

(3) Comparison between the results of Models A, C, D indicates that a high kick velocity during PT can remarkably disrupt the binary systems, resulting in a high birth rate of isolated SS

Table 2. Predicted numbers and birth rates of radio/X-ray SS MSPs with various companion types for different models in the Galaxy.

Model	Phase of MSPs	MS	Gaint	He MS/Gaint	He WD	CO WD	Isolated
A	Radio	291	347	79	30 949	887	5878
		1.5×10^{-6}	4.9×10^{-6}	1.8×10^{-7}	4.3×10^{-6}	1.6×10^{-7}	6.6×10^{-7}
	X-ray	3691	1741	<1	10 905	858	
		1.8×10^{-6}	5.7×10^{-6}	1.1×10^{-7}	9.5×10^{-7}	1.0×10^{-7}	
B	Radio	145	46	14	3446	99	808
		9.8×10^{-7}	1.2×10^{-6}	1.1×10^{-7}	6.3×10^{-7}	3.2×10^{-8}	8.1×10^{-8}
	X-ray	1588	518	<1	2836	267	
		1.2×10^{-6}	1.7×10^{-6}	8.3×10^{-8}	2.4×10^{-7}	2.7×10^{-8}	
C	Radio	146	236	56	35 570	592	0
		1.7×10^{-6}	5.3×10^{-6}	1.1×10^{-7}	4.9×10^{-6}	1.1×10^{-7}	0
	X-ray	3614	1895	<1	11 416	679	
		2.0×10^{-6}	6.4×10^{-6}	6.2×10^{-8}	9.9×10^{-7}	7.9×10^{-8}	
D	Radio	283	241	43	26 841	490	19 862
		1.1×10^{-6}	4.0×10^{-6}	1.0×10^{-7}	3.7×10^{-6}	9.7×10^{-8}	2.1×10^{-6}
	X-ray	3555	1609	<1	10 269	698	
		1.6×10^{-6}	4.8×10^{-6}	7.7×10^{-8}	9.0×10^{-7}	8.1×10^{-8}	
E	Radio	9	29	0	3061	0	852
		3.5×10^{-8}	4.1×10^{-7}	0	4.1×10^{-7}	0	9.8×10^{-8}
	X-ray	142	186	0	942	0	
		1.1×10^{-7}	5.1×10^{-7}	0	1.0×10^{-7}	0	
F	Radio	16	132	<1	12 124	<1	2573
		1.3×10^{-7}	1.6×10^{-6}	2.9×10^{-9}	1.3×10^{-6}	2.3×10^{-9}	2.8×10^{-7}
	X-ray	116	534	<1	631	25	
		1.2×10^{-7}	1.7×10^{-6}	2.9×10^{-9}	5.8×10^{-8}	2.3×10^{-9}	
G	Radio	278	629	70	36 287	767	6702
		1.5×10^{-6}	5.3×10^{-6}	1.7×10^{-7}	4.7×10^{-6}	1.2×10^{-7}	7.5×10^{-7}
	X-ray	3641	1719	<1	9902	703	
		1.7×10^{-6}	5.6×10^{-6}	1.3×10^{-7}	8.6×10^{-7}	9.2×10^{-8}	
I	Radio	68	24	40	2131	418	693
		5.2×10^{-7}	7.8×10^{-7}	9.6×10^{-8}	6.2×10^{-7}	9.1×10^{-8}	7.4×10^{-8}
	X-ray	812	154	<1	4850	594	
		4.2×10^{-7}	9.8×10^{-7}	8.2×10^{-8}	4.2×10^{-7}	7.1×10^{-8}	
J	Radio	3548	817	28	21 009	68	26 308
		8.0×10^{-6}	7.7×10^{-6}	6.2×10^{-8}	4.7×10^{-6}	3.5×10^{-8}	2.4×10^{-6}
	X-ray	32 837	8100	<1	23 961	370	
		1.1×10^{-5}	1.4×10^{-5}	2.5×10^{-8}	2.1×10^{-6}	4.0×10^{-8}	

MSPs, while a low kick velocity with $\sigma_{\rm PT} = 20 {\rm kms}^{-1}$ can hardly disrupt the binary.

(4) Model G predicts similar results to Model A which indicates that, compared to other parameters, the influence of $M_{\rm SS,MAX}$ is minor.

(5) All models predict a considerable SS + He WD binary MSPs, while the predicted birth rates and numbers of other types of SS binary MSPs are much smaller than those of SS + He WD binary MSPs.

4.2. Evolutionary traces and initial parameters

Figure 1 shows the evolutionary traces of the mass of the NS and the donor star, orbital period, and eccentricity for three cases forming isolated MSP, He WD+SS binary MSP, and CO WD+SS binary MSP in Model A. It is easy to find the PT position because of the sudden mass decrease of the NS. In all three cases, the PT takes place during the RLOF stage.

In Fig. 2, the initial 3D parameter-space of $M_{1,\rm i}$, $M_{2,\rm i}$, and $P_{\rm orb,i}$ of the primordial binary systems that can evolve into isolated MSP, He WD + MSP, and CO WD + MSP in Model A are projected onto three planes. The initial parameter distributions of the primordial binary systems forming isolated MSPs are very similar to those of He WD + SS binary MSP and their different evolutionary fates should originate from different kick velocities. However, the primordial binary systems evolving into CO WD + SS binary MSPs prefer to have a relatively heavy secondary star which can be explained by the standard stellar evolutionary model.

4.3. Mass distribution of pulsars

Considering its fast rotation, the mass of SS after PT may stop increasing as a result of the propeller effect. The magnetosphere radius of the SS under the assumption of spherical accretion is $r_{\rm m} = 6.0 \times 10^6 (B_9)^{4/7} |\dot{M}_{17}|^{-2/7}$ cm, where B_9 is the surface magnetic field of SS in units of 10^9 G and $\dot{M}_{17}$ is the accretion rate of SS in units of 10^{17} g s^{-1} (Ghosh & Lamb 1979a,b; Liu & Chen 2011). The corotation radius of the SS can be estimated as:

$$r_{\rm co} = 1.5 \times 10^6 \left(\frac{M_{\rm SS}}{M_\odot}\right)^{1/3} \left(\frac{P}{1\,{\rm ms}}\right)^{2/3} {\rm cm}. \quad (10)$$

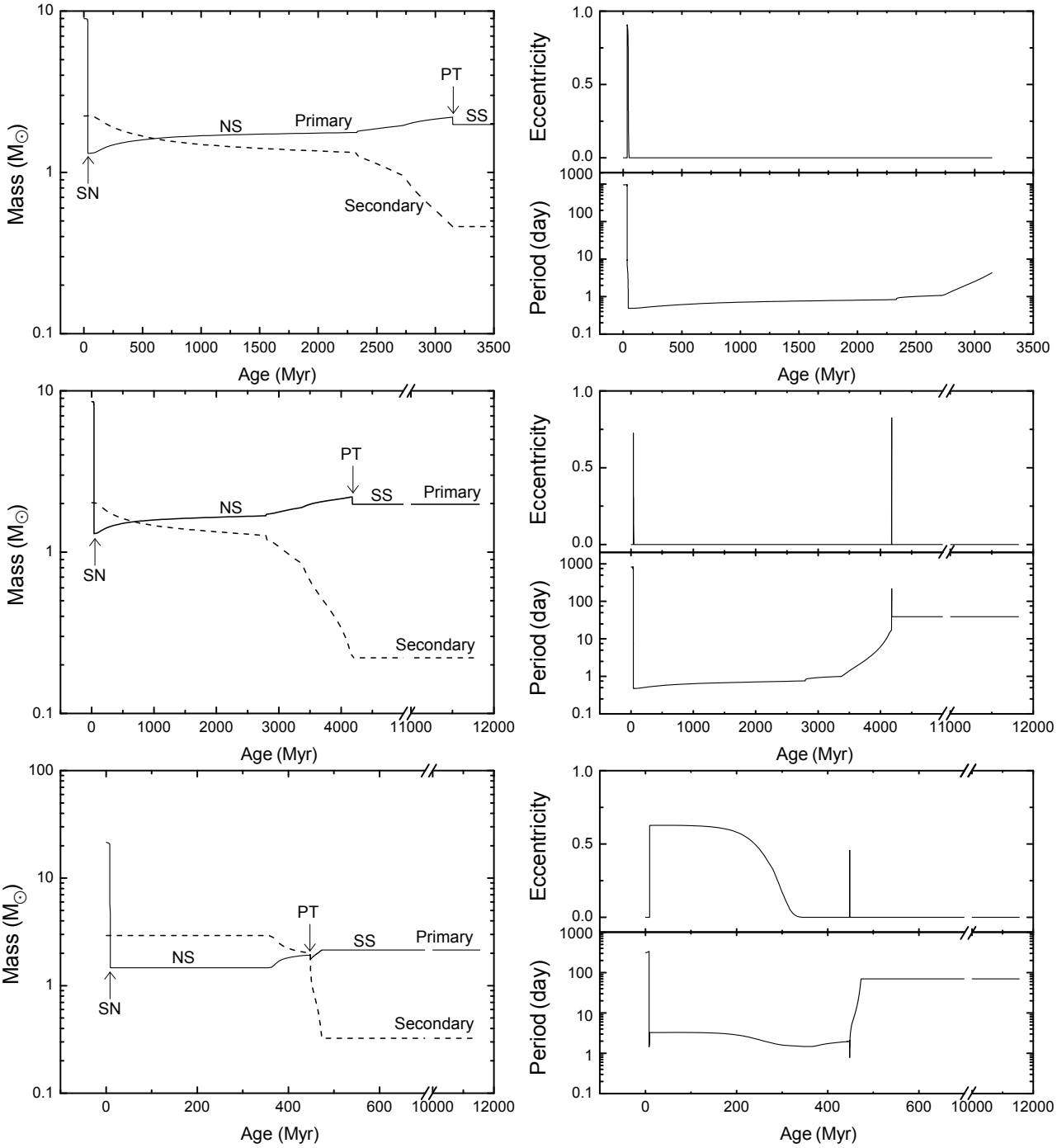

Fig. 1. Evolutionary traces of mass, orbital period, and eccentricity for the three cases which see the evolution into isolated MSP (*top panel*), He WD+ SS MSP binary (*middle panel*), and CO WD+SS MSP binary (*bottom panel*), respectively.

The radius of the object after PT should decrease due to the mass loss. According to the conservation of the magnetic flux, the surface magnetic field of the object would be enhanced, while the spin period would decrease due to the conservation of the angular momentum. As a result, the magnetosphere radius moves outside and the corotation radius moves inside. Therefore, the propeller effect may possibly occur. Taking this possibility into consideration, we also simulate Model H (the twin of Model A, with all input parameters the same as for Model A) for which the mass of SS will no longer increase after PT.

Figure 3 summarizes the simulated mass distributions of various binary MSPs in the Galaxy. The top and bottom panels show the mass distribution of radio (no mass accretion) and X-ray binary MSPs, respectively. The red dashed lines, and black dashed lines represent the number of all binary MSPs (including NS and SS MSPs) predicted by Model A and H, respectively. Since the further accretion after PT process ceases, the maximum mass of MSPs predicted by Model H is 2.2 $M_{\odot}$ (also see Eq. (1)). The dotted lines correspond to SS MSPs predicted by Model A, implying the contribution of core collapse NS obviously exceeds SS for MSPs with a mass of 1.6−2.2 $M_{\odot}$. However, SS evolutionary channel provides the whole contribution for the radio MSPs with a mass exceeding 2.2 $M_{\odot}$. Recent observation revealed that there exists a heavy MSP with a mass of

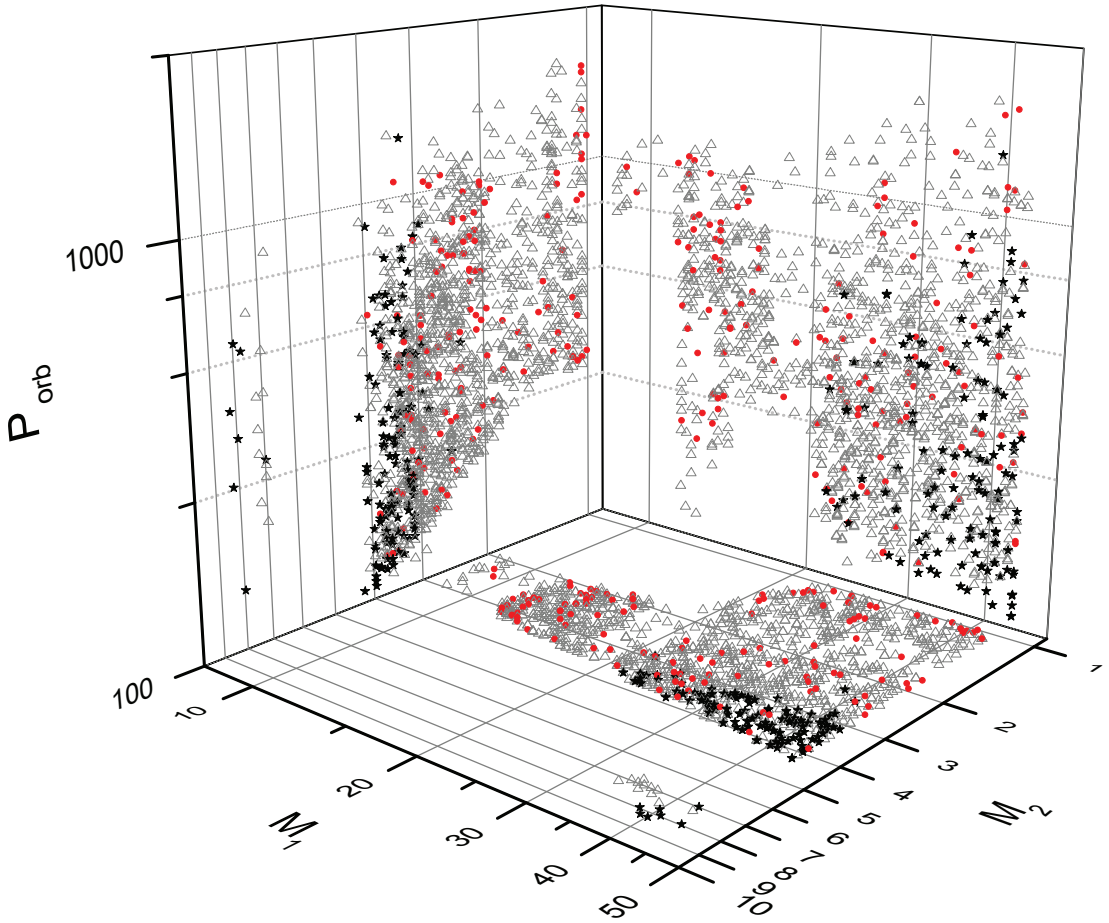

Fig. 2. Projections of the 3D-distribution of the initial primary masses (M_1), the secondary masses (M_2), and orbital periods ($P_{\rm orb}$) of primordial binary systems that would evolve into isolated MSPs (red solid circles), He WD+SS binary MSPs (grey open triangles), and CO WD+ SS binary MSPs (black solid stars), respectively.

2.1 $M_\odot$ (Yap et al. 2019), the NS-SS PT scenario may be responsible for the origin of such a heavy MSP.

4.4. Influence of input parameters

4.4.1. CE parameters

In Fig. 4, the birth rate of SS MSPs is shown as a function of the delay time between the formation of primordial binary systems and the PT. The influence of different CE parameters on the birth rate of all SS MSPs are shown in the top panel. It is clear that Models A, C and D with the same CE parameters lead to a large birth rate of SS MSPs.

4.4.2. Kick velocity

The middle and bottom panels indicate the influence of PT kick on the birth rate of isolates SS MSPs or SS binary MSPs, respectively. It is obvious that a higher kick velocity would easily lead to the disruption of binaries, yielding a relatively higher birth rate of isolated SS MSPs. In addition, as shown in Table 2, when the kick velocity $\sigma_{\rm PT} = 20\,{\rm km\,s^{-1}}$ (Model C), it is difficult to disrupt the binaries and produce isolated SS MSPs. As a result, there is no Model C in the middle panel of Fig. 4.

4.4.3. Maximum mass of SS

When the mass of SS in a binary reaches the maximum mass $M_{\rm SS,MAX}$ during the mass accretion, the SS binary MSP would evolve into a black hole binary and would not contribute to the birth rate of SS binary MSPs. Therefore, a lower maximum mass of SS should result in a lower birth rate of SS binary MSPs. For isolated SS MSPs with no mass transfer after PT, the birth rate is irrelevant to the maximum mass of SS. The minor difference of birth rates and number of isolated SS MSPs shown in Table 2 should arise from different random numbers.

The integrated number distribution of binary radio MSPs (including NS and SS) predicted by Model A and G are shown in Fig. 5. Comparing the difference between models A and G in Table 2 and Fig. 5, the influence of the maximum mass on the birth rates and numbers of SS binaries with different companion types can be more or less neglected if we deduct the factor of the random numbers. The arrow in Fig. 5 indicates the cutoff point for the integrated mass distribution and total number of radio MSPs when $M_{\rm SS,MAX} = 2.2\,M_\odot$ (other input parameters are same to models A and G).

4.4.4. Accretion efficiency

As shown in Table 2, the accretion efficiency $f_{\rm acc}$ can significantly influence the simulated results. Generally, a higher accretion efficiency always results in higher birth rates and numbers of isolated SS MSPs. However, for binary SS MSPs with different companion types, the influence tendency is complicated. The accretion process would influence the orbital evolution of the binary system, resulting in different orbital periods and donor-star masses; hence, it would produce different

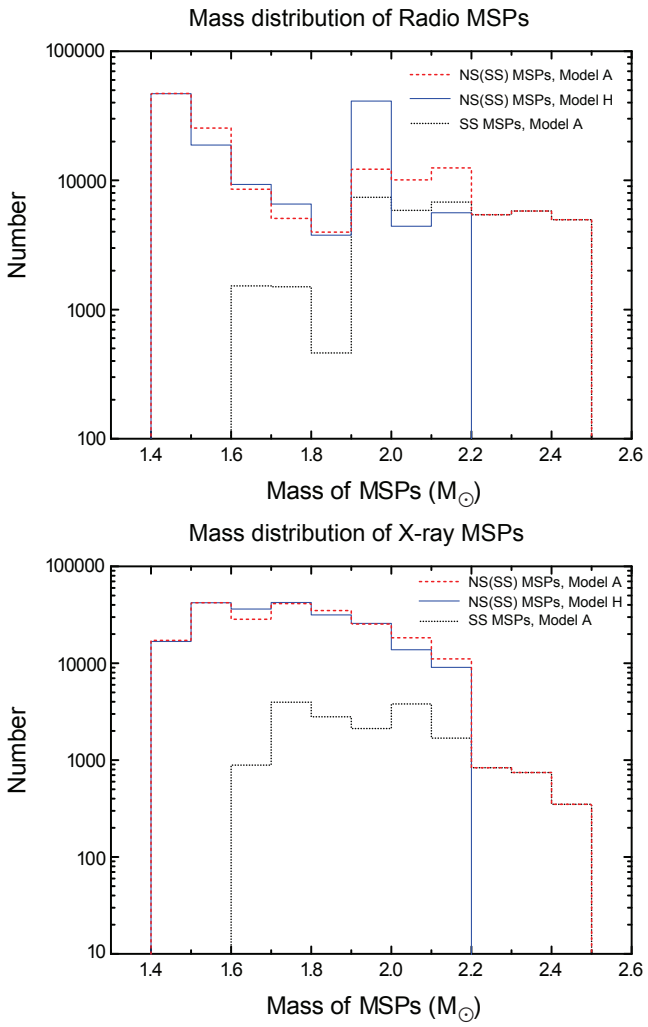

Fig. 3. Mass distribution of radio (*top panel*) and X-ray (*bottom panel*) MSPs in our simulated binaries in the Galaxy. The red dashed lines and black dashed lines represent the number of all binary MSPs (including NS and SS MSPs) predicted by Model A and H (twin of A, see Sect. 4.3, for detail), respectively. The dotted lines correspond to SS MSPs predicted by Model A.

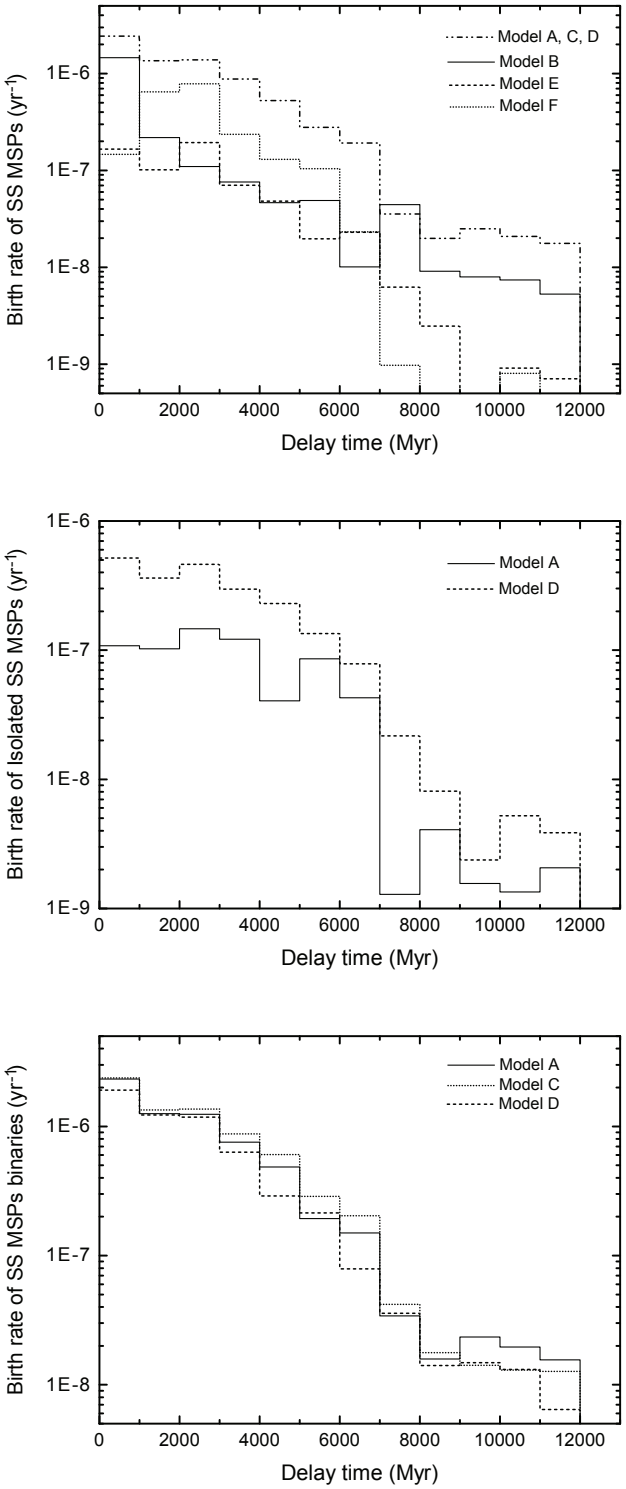

Fig. 4. Birth rate versus delay time. *Top panel*: influence of CE parameters on the birth rate of all SS MSPs; *middle panel*: influence of PT kick velocity on the formation of isolated SS MSPs; *bottom panel*: influence of PT kick velocity to the formation of SS binary MSPs.

birth rates and numbers of binary SS MSPs with different companion types.

5. Discussion

5.1. Eccentric binary MSPs

As mentioned above, in our simulation all PT processes take place during the RLOF and the orbital circularization is very rapid due to the following mass exchange (as shown in the right middle and bottom panels of Fig. 1). Therefore, it seems difficult to produce eccentric He WD + MSP binaries, which are very rare in the Galaxy. However, (1) the PT will occur if the mass of the NS is larger than $M_c(\Omega)$ during the spin-down process[2] and (2) it is possible that the PT processes take place at the final stage of the mass transfer (at the endpoint of RLOF or the time scale of the following mass transfer after PT is very short). These terms indicate that the MSPs with He WD companions in eccentric orbit may originate from NS-SS PT. Jiang et al. (2015) has already proposed a NS-SS PT model to account for the eccentric binary MSPs which arised from the sudden loss of the gravitational mass of the NS during the PT.

Apart from the NS-SS PT scenario, some other models can also account for the formation of eccentric binary MSPs.

[2] Since the magnetic fields of MSPs are very weak, we ignore the spin-down process that is due to the magnetic dipole radiation in the simulation.

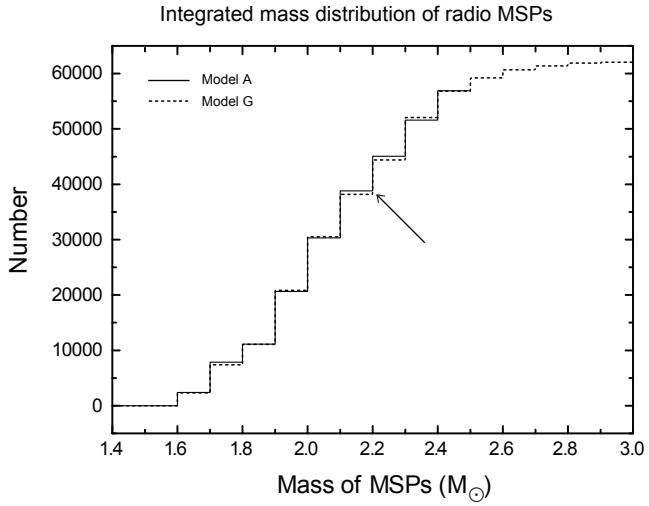

Fig. 5. Integrated number distribution of MSPs mass in radio binaries predicted by Model A (solid line) and G (dashed line), while the arrow indicates the cutoff with $M_{\rm SS,MAX} = 2.2\,M_\odot$

Antoniadis (2014) suggests that the dynamical interaction between the binary and a circumbinary disk (CB disk) could result in an eccentricity of $e \sim 0.01-0.15$ for He WD binary MSPs with orbital periods between 15 and 50 days.

The scenario of delayed accretion-induced collapse (AIC) of accreting massive WD first proposed by Michel (1987) has been widely studied by different authors (Ivanova & Taam 2004; van Paradijs et al. 1997; Xu & Li 2009; Hurley et al. 2010). Freire & Tauris (2014) suggest that the orbital eccentricity may be caused by a sudden mass loss during AIC. Population-synthesis simulation given by Chen et al. (2011) shows that the AIC scenario can also produce enough isolated MSPs in the Galaxy. Barr et al. (2017) report the measurement of both the advance of periastron and the Shapiro delay for PSR J1946+3417 and obtain the mass of the pulsar, which is 1.828(22) $M_\odot$. Since the Chandrasekhar mass of the WD is 1.4 $M_\odot$, the mass of the MSP forming by the AIC channel should be ~1.2 $M_\odot$. Even if we consider the collapse of a super-Chandrasekhar mass WD, it is difficult to form such a heavy MSP[3].

5.2. MSPs with warm surfaces

Some MSPs are reported to have relatively high surface temperatures, which are not consistent with their cooling evolution. For example, the spectrum of PSR J0437-4715 and the WD companion can be fit with surface temperatures of $\sim 10^5$ K and ~4000 K, respectively (Durant et al. 2012). The optical-far-UV spectrum of isolated MSP J2124-3358, observed by the *Hubble* Space Telescope, constrained its surface temperature at $\sim 10^5$ K (Rangelov et al. 2017). Considering the heating process during PT, the anomalous surface temperatures of PSR J0437-4715 and J2124-3358 can be interpreted by NS-SS PT scenario, similarly to the double WD binary SDSS J125733.63+542850.5 studied by Jiang et al. (2018).

6. Summary

In this work, we propose a NS-SS PT scenario to interpret the origin of isolated MSPs. Once the mass of the NS exceeds the maximum mass due to the accretion, the NS-SS PT process occurs and a suitable kick would disrupt the binary, resulting in the birth of isolated MSPs. Employing the population-synthesis code, we simulate the evolution of 8×10^6 binary systems for several models with different input parameters λ, $\alpha_{\rm CE}$, $\sigma_{\rm PT}$, $M_{\rm SS,MAS}$ and $f_{\rm acc}$. The simulated results show that the NS-SS PT scenario with a kick velocity of $\sigma_{\rm PT} = 60\,{\rm km\,s^{-1}}$ can produce a considerable isolated MSPs, which is approximately in agreement with the predictions given by Lorimer (1995), Lyne et al. (1998), Ferraio & Wickramasinghe (2007), Story et al. (2007). Meanwhile, disrupted binary MSPs with He WDs should be responsible for the origin of isolated low mass He WDs, which cannot evolve from the normal single star evolutionary channel (Wang & Han 2009; Zorotovic & Schreiber 2017). In the present scenario, most donor stars, companions of the progenitors of isolated SS MSPs, would evolve into He WDs in the Hubble time, hence, the upper limit of birth rate of isolated low-mass He WDs via NS-SS PT should be similar to that of isolated MSPs. In addition, the scenario also predicts considerable He WD + SS binary MSPs and the mass distribution of MSPs can be used to check the current scenario.

At present, the predicted NS-SS PT event has never been confirmed by observation. In principle, current transient surveys may hint at some SS candidates. An NS-SS PT event could be observed as short γ-ray burst (Cheng & Dai 1996) or quark-nova (Ouyed et al. 2002), releasing 10^{53} ergs in a short timescale (less than one second). Recently, Yu et al. (2019) predicted that the accretion-induced collapse (AIC) of white dwarfs should be associated with recently discovered fast-evolving luminous transients (Yu et al. 2015), which has been observed in all of the optical, soft, and hard X-ray bands. If the NS-SS PT process produces a highly magnetized MSPs, the observed phenomenon should be similar to the AIC. Certainly, the mass of SS MSPs should be greater than that of MSPs forming by AIC.

Acknowledgements. We thank the referee for a very careful reading and comments that have led to the improvement of the manuscript. This work was supported by the CAS "Light of West China" Program (Grants No. 2018-XBQNXZ-B-022) and the National Natural Science Foundation of China (Grant Nos. 11573016, 11733009, 11773015, 11803018, U1731103, 11463004 and 11605110), the National Key Research and Development Program of China (Grant No. 2016YFA0400803 and 2016YFA0400804), the Scientific Research Fund of Hunan Provincial Education Department (Grant Nos. 16B250 and 16C1531), and the Program for Innovative Research Team (in Science and Technology) at the University of Henan Province.

References

Akmal, A., Pandharipande, V. R., & Ravenhall, D. G. 1998, Phys. Rev. C, 58, 1804
Alcock, C., Farhi, E., & Olinto, A. 1996, ApJ, 310, 261
Alpar, A., Cheng, A. F., Ruderman, M. A., & Shaham, J. 1982, Nature, 300, 728
Antoniadis, J. 2014, ApJ, 797, L24
Baym, G., Pethick, C., & Sutherland, P. 1971, ApJ, 170, 299
Barr, E. D., Freire, P. C. C., Kramer, M., et al. 2017, MNRAS, 465, 1711
Berezhiani, Z., Bombaci, I., Drago, A., et al. 2003, ApJ, 586, 1250
Bhattacharya, D., & van den Heuvel, E. P. J. 1991, Phys. Rep., 203, 1
Bhattacharyya, S., Bombaci, I., Logoteta, D., & Thampan, A. V. 2017, ApJ, 848, 65
Bodmer, A. R. 1971, Phys. Rev. D, 4, 1601
Bombaci, I., & Datta, B. 2000, ApJ, 530, L69
Bombaci, I., Parenti, I., & Vidaña, I. 2004, ApJ, 614, 314
Bombaci, I., Panda, P. K., Providência, C., & Vidaña, I. 2008, Phys. Rev. D, 77, 083002
Bombaci, I., Logoteta, D., Vidaña, I., & Providência, C. 2016, Eur. Phys. J. A, 52, 58
Chen, W.-C., & Li, X.-D. 2009, ApJ, 702, 686
Chen, W.-C., Liu, X.-W., Xu, R.-X., & Li, X.-D. 2011, MNRAS, 410, 1441
Chen, H.-L., Chen, X., Tauris, T. M., & Han, Z. 2013, ApJ, 775, 27

[3] According to the simulation given by Chen & Li (2009), the massive WD exceeding 2.0 $M_\odot$ cannot be produced by the mass accretion.

Cheng, K. S., & Dai, Z. G. 1996, Phys. Rev. Lett., 77, 1210
Cheng, K. S., & Zhang, C. M. 2000, A&A, 361, 1001
de Kool, M. 1990, ApJ, 358, 189
Dewi, J. D. M., & Tauris, T. 2000, A&A, 360, 1043
Dewi, J. D. M., & Pols, O. R. 2003, MNRAS, 344, 629
Dey, M., Bombaci, I., Dey, J., et al. 1998, Phys. Lett. B, 438, 123
Drago, A., Lavagno, A., & Parenti, I. 2007, ApJ, 659, 1519
Durant, M., Kargaltsev, O., Pavlov, G. G., et al. 2012, ApJ, 746, 6
Farhi, E., & Jaffe, R. L. 1984, Phys. Rev. D, 30, 2379
Ferraio, L., & Wickramasinghe, D. 2007, MNRAS, 375, 1009
Freire, P. C. C., & Tauris, T. M. 2014, MNRAS, 438, 86
Fruchter, A. S., Stinebring, D. R., & Taylor, J. H. 1988, Nature, 333, 237
Gangopadhyay, T., Ray, S., Li, X.-D., et al. 2013, MNRAS, 431, 3216
Ghosh, P., & Lamb, F. K. 1979a, ApJ, 232, 259
Ghosh, P., & Lamb, F. K. 1979b, ApJ, 234, 296
Glendenning, G. K. 2000, Compact Stars (New York: Springer)
Haensel, P., & Yakovlev, D. G. 2007, Neutron Stars 1: Equation of State and Structure (Springer)
Haensel, P., Zedunik, J. L., & Schaeffer, R. 1986, A&A, 160, 121
Hartle, J. B. 1970, ApJ, 161, 111
Hills, J. G. 1983, ApJ, 267, 322
Hobbs, G., Lorimer, D. R., Lyne, A. G., & Kramer, M. 2005, MNRAS, 360, 974
Horvath, J. E., & Benvenuto, O. G. 1988, Phys. Lett. B, 213, 516
Hurley, J. R., Pols, O. R., & Tout, C. A. 2000, MNRAS, 315, 543
Hurley, J. R., Tout, C. A., & Pols, O. R. 2002, MNRAS, 329, 897
Hurley, J. R., Tout, C. A., Wickramasinghe, D. T., et al. 2010, MNRAS, 402, 1437
Itoh, N. 1970, Prog. Theor. Phys., 44, 291
Ivanova, N., & Taam, R. E. 2004, ApJ, 601, 1058
Jia, K., & Li, X.-D. 2016, ApJ, 830, 153
Jiang, L., Li, X.-D., Dey, J., & Dey, M. 2015, ApJ, 807, 41
Jiang, L., Chen, W.-C., & Li, X.-D. 2018, MNRAS, 476, 109
Kluzniak, W., Ruderman, M., Shaham, J., & Tavani, M. 1988, Nature, 334, 225
Kroupa, P., Tout, C. A., & Gilmore, G. 1993, MNRAS, 262, 545
Lai, X.-Y., & Xu, R.-X. 2009, MNRAS, 398, L31
Lasota, J.-P., Haensel, P., & Abramowicz, M. A. 1996, ApJ, 456, 300
Liu, X.-W., & Li, X.-D. 2006, A&A, 449, 135
Liu, X.-W., & Li, X.-D. 2007, Chin. J. Astron. Astrophys., 7, 389
Liu, W.-M., & Chen, W.-C. 2011, MNRAS, 416, 2285
Lorimer, D. R. 1995, MNRAS, 274, 300
Lorimer, D. R. 2008, Liv. Rev. Rel., 11, 8
Lyne, A. G., Manchester, R. N., Lorimer, D. R., et al. 1998, MNRAS, 295, 743
Manchester, R. N. 2004, Science, 304, 542
Marquez, K. D., & Menezes, D. P. 2007, JCAP, 12, 028
Michel, F. C. 1987, Nature, 329, 310
Morrison, I. A., Baumgarte, T. W., & Shapiro, S. L. 2004, ApJ, 610, 941
Olinto, A. V. 1987, Phys. Lett. B, 192, 71
Ouyed, R., Dey, J., & Dey, M. 2002, A&A, 390, L39
Phinney, E.S. 1992, Phil. Trans. R. Soc. London Ser. A Phys. Eng. Sci., 341, 39
Podsiadlowski, P., Rappaport, S., & Pfahl, E. D. 2002, ApJ, 565, 1107
Podsiadlowski, P., Rappaport, S., & Han, Z. 2003, MNRAS, 341, 385
Pylyser, E., & Savonije, G. J. 1989, A&A, 208, 52
Radhakrishnan, V., & Srinivasan, G. 1982, Curr. Sci., 51, 1096
Rangelov, B., Pavlov, G. G., Kargaltsev, O., et al. 2017, ApJ, 835, 264
Schaffner-Bielich, J., Hanauske, M., Stöcker, H., & Greiner, W. 2002, Phys. Rev. Lett., 89, 171101
Shannon, R. M., Cordes, J. M., Metcalfe, T. S., et al. 2013, ApJ, 766, 5
Shao, Y., & Li, X.-D. 2016, ApJ, 816, 45
Staff, J. E., Ouyed, R., & Jaikumar, P. 2006, ApJ, 645, L145
Story, S. A., Gonthier, P. L., & Harding, A. K. 2007, ApJ, 671, 713
Tout, C. A., Aarseth, S. J., Pols, O. R., & Eggleton, P. P. 1997, MNRAS, 291, 732
van den Heuvel, E. P. J., & van Paradijs, J. 1988, Nature, 334, 227
van Paradijs, J., van den Heuvel, E. P. J., Kouveliotou, C., et al. 1997, A&A, 317, L9
Verbunt, F. 1988, Adv. Space Res., 8, 529
Verbunt, F., van den Heuvel, E. P. J., van Paradijs, J., & Rappaport, S. A. 1987, Nature, 329, 312
Wang, B., & Han, Z. 2009, A&A, 508, L27
Wang, C., Jia, K., & Li, X.-D. 2016, Res. Astron. Astrophys., 16, 126
Webbink, R. F. 1984, ApJ, 277, 355
Witten, E. 1984, Phys. Rev. D, 30, 272
Wolszczan, A., & Frail, D. A. 1992, Nature, 355, 145
Xu, X.-J., & Li, X.-D. 2009, A&A, 495, 243
Xu, X.-J., & Li, X.-D. 2010a, ApJ, 716, 114
Xu, X.-J., & Li, X.-D. 2010b, ApJ, 722, 1985
Yap, Y. X., Li, K. L., Kong, A. K. H., et al. 2019, A&A, 621, L9
Yu, Y.-W., Li, S.-Z., & Dai, Z.-G. 2015, ApJ, 806, L6
Yu, Y.-W., Chen, A., & Li, X.-D. 2019, ApJ, 877, L21
Zhu, C.-H., Lü, G.-L., Wang, Z.-J., & Liu, J.-Z. 2013, PASP, 125, 25
Zorotovic, M., & Schreiber, M. R. 2017, MNRAS, 466, L63